Island-arc basalt alkali ratios: Constraints from phengite-fluid partitioning experiments

Stefan Melzer*
Bernd Wunder — GeoForschungsZentrum Potsdam, Telegrafenberg, 14473 Potsdam, Germany

ABSTRACT

In order to constrain the large ion lithophile (LIL) element distribution for subduction-zone environments, exchange coefficients $K_D^{phe\text{-}fluid} = (X_{Rb,Cs}^{phe} \cdot X_K^{fluid})/(X_K^{phe} \cdot X_{Rb,Cs}^{fluid})$ for K, Rb, and Cs between aqueous fluids and phengite (phe) have been determined experimentally at 2.0 and 4.0 GPa. Derived K_D values for the Rb-K exchange slightly increase from 1.62 ± 0.10 at 2 GPa, 600 °C, to 1.84 ± 0.15 at 4 GPa, 700 °C. For the Cs-K exchange, much lower K_D values of 0.22 ± 0.06 (at 2 GPa, 600 °C) and 0.37 ± 0.10 (at 4 GPa, 700 °C) were determined. The results show that, for the pressure-temperature range investigated, Rb preferentially fractionates into phengite, whereas Cs partitions into the fluid.

Assuming a one-step model of perfect Rayleigh fractionation for continuous decomposition of phengite during subduction, varying alkali ratios observed for island-arc basalts as a function of slab depth may be explained by the LIL-fractionation behavior between fluids and phengites determined in this study. Our data indicate that previously derived models for metasomatic mass transfer during subduction processes need to be reconsidered.

Keywords: phengite, LIL-fractionation, subduction zone, exchange coefficients.

INTRODUCTION

Knowledge of petrological processes taking place during subduction is important not only for a better understanding of the magma production at active plate margins but also for the understanding of element cycles during processes of crustal destruction and formation (Gill, 1981). The large ion lithophile (LIL) elements K, Rb, and Cs are suggested to be important geochemical tracers for subduction-zone environments. The typical enrichment of these LIL elements in island-arc basalts (IAB) relative to mid-ocean ridge basalts (MORB) is thought to be due to the transport of LIL elements from the subducted slab into the arc by metasomatic fluids and/or melts (Fig. 1; e.g., Gill, 1981). Fluids derived from the breakdown of OH-containing minerals within the slab during the subduction process are water rich, carrying mainly silica and LIL elements. Important minerals that may act as sources and sinks of structurally bound water in the subducted slab are amphiboles and micas. Because Rb and Cs structurally may replace K within these minerals, cross-arc geochemical variations of LIL elements (Fig. 1), observed as a function of the depth of the Benioff zone (e.g., Ryan et al., 1995), may be influenced by the fractionation behavior of Cs, Rb, and K between fluid (and melts) and the LIL element-hosting minerals at different slab depths.

Phengites are proposed to be the main host of LIL elements in metasedimentary and metabasaltic blueschists and eclogites. Experimental studies on the stability of phengitic muscovite (Schmidt, 1996; Domanik and Holloway, 1996) indicated that K mica persists to depths much greater than the zone of melt generation (80–150 km) beneath arcs. As mentioned by Domanik and Holloway (1996, p. 4133), "This [the extended phengite stability] requires a mechanism of partitioning of LIL-elements into migrating fluids rather than the simple dehydration of phengite beneath arcs in order to provide for the transfer of these slab signature elements from phengite into arc magmas."

Experimentally determined partitioning coefficients of LIL elements between fluids and minerals at high pressures and temperatures (e.g., Brenan et al., 1995; Stalder et al., 1998) are rare and have not been available for phengite until now. However, such data are highly desirable for a quan-

titative understanding and for modeling (Ayers, 1998) of subduction-zone–related metasomatic mass-transfer processes.

The major goal of this paper is to determine partitioning coefficients of Cs, Rb, and K between aqueous fluid and phengitic muscovite at high pressures by exchange experiments. The results will help to constrain how these elements may be transferred from the slab into the overlying mantle wedge. We investigated the pressure range 2–4 GPa, which corresponds to the typical depth of the subducted slab beneath the volcanic front in island arcs (e.g., Tatsumi, 1986).

EXPERIMENTAL TECHNIQUE

Experimental techniques are only briefly documented herein; see Wunder et al. (1999) for more details. Synthesis experiments were performed at 2.0 GPa, 600 °C and 4.0 GPa, 700 °C in piston cylinder presses. Phengites were synthesized from oxide mixtures and 2 molal aqueous chloride solutions, which contained the exchangeable cations in excess. For each of the two different pressure-temperature conditions, 10 experiments with varying (containing Cs or Rb) fluid/solid ratios were performed (Table 1[1]). The synthesis followed the exchange technique, a detailed description of which was given by Zimmermann et al. (1997). This technique was chosen to avoid the formation of metastable assemblages due to fractional crystallization (Zimmermann et al., 1997). After the fast quench of the experiment (samples cooled below 150 °C in <10 s) the capsule was opened and the fluid extracted. No evidence for quench crystallization, which could affect the fluid composition with respect to the alkalies, was found in any of the runs. The low concentration of alkalies within the fluid guarantees that all dissolved alkalies remain in the fluid during quenching. The fluid was analyzed by inductively coupled plasma–atomic-emission spectroscopy (ICP-AES) for K and Rb and by ICP-MS (mass spectroscopy) for its Cs contents. The solid products were characterized optically and by scanning electron microscopy (SEM). The composition was determined by routine electron microprobe (EMP) analyses. Polished samples were analyzed with

---

[1]GSA Data repository item 200065, Appendix Tables 1 and 2, Starting mixtures and phengite analyses, is available on request from Documents Secretary, GSA, P.O. Box 9140, Boulder, CO 80301-9140, editing@geosociety.org, or www.geosociety.org/pubs/ft2000.htm.
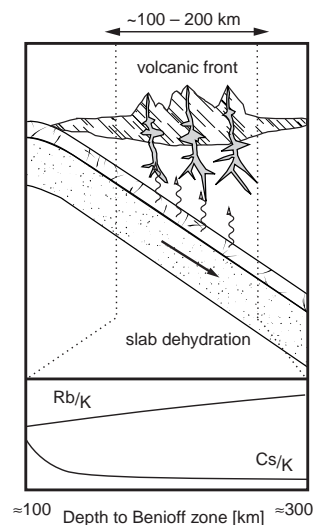
Figure 1. Schematic model showing process of dehydration below volcanic front at convergent plate margins. Systematic variations of alkali-element ratios (Rb/K, Cs/K) in volcanic magmas across island arc (Hutchison, 1976; Ryan et al., 1995) give evidence that fluids derived from subducted slab at depth between 100 and 300 km influence alkali-element budget of island-arc basalts.

*E-mail: smelzer@gfz-potsdam.de.

Data Repository item 200065 contains additional material related to this article.

TABLE 1. CHEMICAL COMPOSITIONS OF PHENGITES AND COEXISTING FLUIDS																				
Run number	1	2	82[†]	84[†]	85	37	55	57	63	76	5	7	8	9	10	59	60	62	78	79
Run duration [d]	6	6	4	5	5	2	4	4	2	4	6	6	6	6	6	3	3	3	4	4
Run conditions	2 GPa, 600 °C					4 GPa, 700 °C					2 GPa, 600 °C					4 GPa, 700 °C				
Phases [wt%]																				
1M phengite	26	37	35	38	25	19	14	10	1	15	33	25	23	34	31	31	17	29	17	18
2M₁ phengite	53	53	57	62	68	54	64	63	52	72	61	70	77	43	68	44	59	63	46	68
quartz / coesite	21	10	8		7	18	13	14	21	1	6	5		23	1	16	15	4	19	9
kyanite						9	9	13	26	12						9	9	3	19	7
Phengite composition[#]																				
Si	3.66	3.62	3.58	3.64	3.47	3.73	3.59	3.61	3.61	3.63	3.43	3.49	3.52	3.43	3.46	3.68	3.70	3.61	3.67	3.65
Al	1.86	1.86	1.93	1.88	2.10	1.70	1.89	1.83	1.90	1.90	2.27	2.11	2.04	2.27	2.12	1.81	1.82	1.89	1.82	1.86
Mg	0.51	0.55	0.52	0.48	0.49	0.64	0.55	0.61	0.51	0.47	0.40	0.48	0.48	0.36	0.46	0.52	0.49	0.53	0.54	0.50
K	0.66	0.42	0.84	0.76	0.57	0.47	0.74	0.63	0.81	0.78	0.59	0.77	0.81	0.69	0.85	0.79	0.68	0.64	0.75	0.57
Rb	0.10	0.45	0.03	0.11	0.25	0.25	0.14	0.22	0.06	0.07	0.00	0.00	0.00	0.00	0.00	0.00	0.00	0.00	0.00	0.00
Cs	0.00	0.00	0.00	0.00	0.00	0.00	0.00	0.00	0.00	0.00	0.06	0.01	0.01	0.04	0.05	0.00	0.00	0.19	0.03	0.25
X_K	0.87	0.48	0.97	0.88	0.70	0.65	0.84	0.74	0.93	0.91	0.91	0.99	0.99	0.95	0.95	0.97	0.89	0.77	0.96	0.69
X_{Rb}	0.13	0.52	0.03	0.12	0.30	0.35	0.16	0.26	0.07	0.09	0.00	0.00	0.00	0.00	0.00	0.00	0.00	0.00	0.00	0.00
X_{Cs}	0.00	0.00	0.00	0.00	0.00	0.00	0.00	0.00	0.00	0.00	0.09	0.01	0.01	0.05	0.05	0.03	0.11	0.23	0.04	0.31
Fluid composition																				
X_K	0.89	0.61	0.98	0.94	0.76	0.79	0.89	0.83	0.94	0.92	0.72	0.93	0.92	0.77	0.68	0.78	0.56	0.58	0.90	0.44
X_{Rb}	0.11	0.39	0.02	0.06	0.24	0.21	0.11	0.17	0.06	0.08	0.00	0.00	0.00	0.00	0.00	0.00	0.00	0.00	0.00	0.00
X_{Cs}	0.00	0.00	0.00	0.00	0.00	0.00	0.00	0.00	0.00	0.00	0.28	0.07	0.08	0.23	0.32	0.22	0.44	0.42	0.10	0.56

[†]Analytical sum < 85%.

[#]Cation proportions normalized to 11 oxygens and based on average electron microprobe analyses. Full analyses are available in the GSA Data Repository item 200065 (see footnote 1).

Cameca SX50 and SX100 microprobes equipped with wave-length dispersive systems. Counting times for all elements were 20 s on the peak position and 10 s on the background of each side of the peak. Operating conditions were 15 kV and 20 nA. Significant losses of alkalies were not observed during the analysis. Repeated measurements on the same point result in identical alkali concentrations. In addition, for quantitative phase analysis, X-ray powder diffraction patterns (XRD) of all solid products were collected.

RESULTS

Results of synthesis-exchange experiments are summarized in Table 1. Run products consisted predominantly of phengitic mica. Additional phases are quartz in the 2 GPa run and coesite and kyanite in the 4 GPa run. Phase proportions as determined by XRD are listed in Table 1. Grain sizes of micas formed at 2 GPa are rather small, often <10 μm in diameter and <1 μm in thickness. At pressures of 4 GPa, micas are significantly larger, forming platelets to 40 μm in diameter. Most EMP analyses of phengite synthesized at 2 GPa have totals below 70 wt% and were therefore rejected. Only analyses with totals >85 wt% were used for the determination of the phengite composition (exceptions are phengites of runs 82 and 84; see Table 1). For phengites synthesized at 4 GPa, EMP analyses mostly resulted in totals >90 wt% for all runs. Chemical variations within each run are rather small, indicating only one population of phengite. Chlorine was not detected in any of the analyses.

Normalized to 11 oxygens, micas show phengitic compositions in the range of $(K, Rb, Cs)^{XII}_{0.81 \pm 0.06} (Al_{1.53 \pm 0.07} Mg_{0.50 \pm 0.06})^{VI}_{2.04 \pm 0.03} (Al_{0.41 \pm 0.09} Si_{3.59 \pm 0.09})^{IV}_4 (O_{10}/[OH]_2)$. For the Rb-K series phengites with mole fractions $X^{phe}_{Rb} = Rb/(K + Rb)$ in the range of 0.03–0.52 at 2 GPa and 0.07–0.35

at 4 GPa were produced. The X^{fluid}_{Rb} values of the coexisting fluid were in the range 0.02–0.39 (at 2 GPa) and 0.06–0.21 (at 4 GPa), respectively. Phengites from the Cs-K series have mole fractions $X^{phe}_{Cs} = Cs/(K + Cs)$ of $0.01 \leq X^{phe}_{Cs} \leq 0.09$ at 2 GPa and of $0.03 \leq X^{phe}_{Cs} \leq 0.31$ at 4 GPa. For the coexisting fluid X^{fluid}_{Cs} is significantly higher (0.07–0.32, at 2 GPa; 0.10–0.56 at 4 GPa).

The element partitioning of Rb-K and Cs-K between phengite and fluid is shown in Figure 2 as reciprocal ternaries. Within the analytical errors, the tie lines between phengite and the coexisting fluid are internally consistent; only minor crosscutting occurs and the tie lines are close to the bulk composition. This strongly suggests that chemical equilibrium has been attained and that equilibrium exchange coefficients K_D may have been approached in our experiments. Some tie lines miss the bulk composition because of analytical errors and due to the formation of additional phases (Table 1). This is supported by the fact that only one population of phengite is present in each experiment. Fractional crystallization during the course of the synthesis would lead to varying phengite compositions, which were not observed. From Figure 2 it becomes evident that, at each of the experimental conditions, Rb partitions into the phengite relative to K, whereas Cs strongly fractionates into the coexisting fluid. The resulting Rb-K and Cs-K partitionings between phengites and aqueous fluids are presented in $X^{phe}_{Rb} - X^{fluid}_{Rb}$ and $X^{phe}_{Cs} - X^{fluid}_{Cs}$ plots in Figure 3. Strong deviations from the ideal exist for both the Rb-K and Cs-K partitioning. Exchange coefficients are defined by:

$$K_D^{Rb,Cs-K}(\text{phe-fluid}) = \frac{\left(X^{phe}_{Rb,Cs} / X^{fluid}_{Rb,Cs}\right)}{\left(X^{phe}_K / X^{fluid}_K\right)}. \quad (1)$$
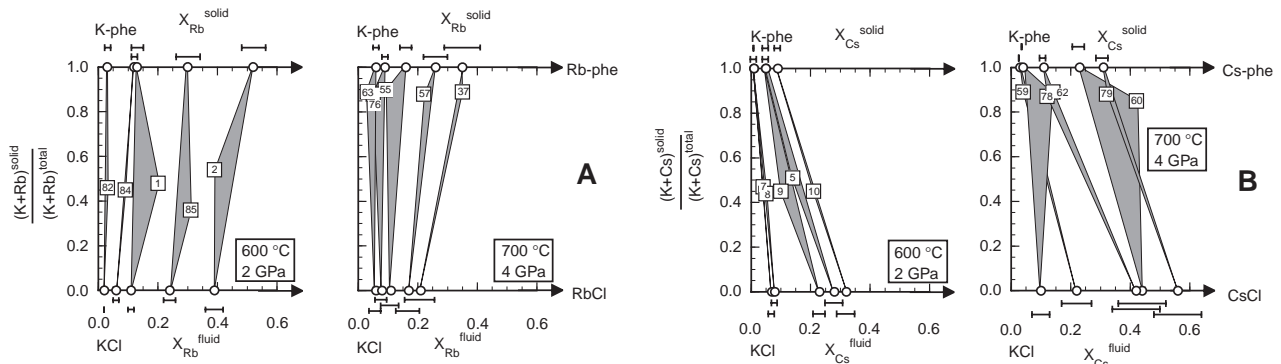

Figure 2. Reciprocal ternary diagrams showing (A) Rb-K and (B) Cs-K distribution between mica and fluid. Squares show bulk compositions and circles show compositions of coexisting phengites and fluid. Tie lines between product phengite and fluid close to bulk composition indicate chemical equilibrium. Error bars correspond to compositional range of electron microprobe analyses for phengite, and to 3% relative errors for fluid. Estimated errors for bulk composition are smaller than symbol size.
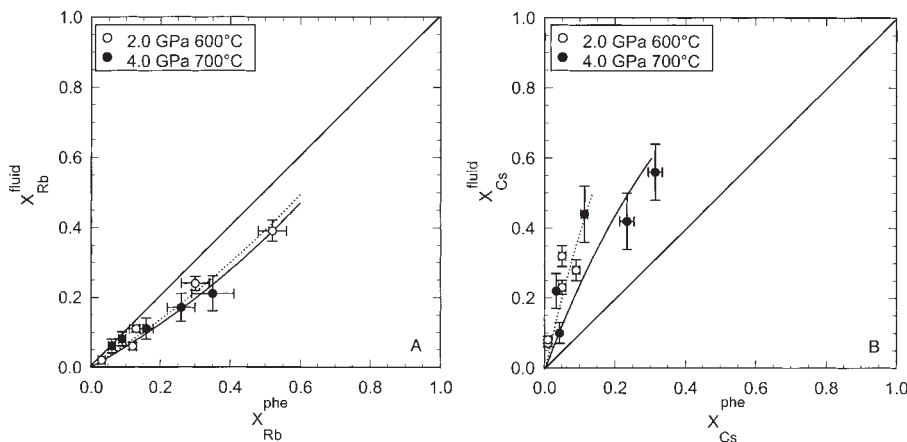
Figure 3. Experimental results in terms of (A) X_{Rb}^{phe} versus X_{Rb}^{fluid} and (B) X_{Cs}^{phe} versus X_{Cs}^{fluid}. Solid curves through data points show fitted Rb-K and Cs-K partitioning between phengite and fluid for experiments performed at 4.0 GPa; dotted line is for experiments performed at 2.0 GPa. Pressure effects are small. Straight line indicates ideal mixing curve.

It is evident from Figure 3 that Henry's law is valid for low Rb and Cs concentrations ($X_{Rb}^{phe}, X_{Cs}^{phe} < 0.1$). Therefore, constant exchange coefficients were determined (Table 2) by using the fitted curves and extrapolating these data to Rb and Cs concentrations of the parts per million range, which is relevant for nature. Based on these derived K_D values, the exchange coefficient for Cs-Rb (Table 2) was calculated according to

$$K_D^{Cs-Rb}(\text{phe-fluid}) = \frac{K_D^{Cs-K}}{K_D^{Rb-K}}. \quad (2)$$

Calculated partition coefficients $D_{Rb,Cs}^{phe-fluid} = c_{Rb,Cs}^{phe}/c_{Rb,Cs}^{fluid}$ for Rb and Cs are also listed in Table 2. However, D values strongly depend on the molalities of the chloridic solution, whereas the exchange coefficient K_D does not.

DISCUSSION

The formation of phengite will drastically alter the K/Rb, K/Cs, and Cs/Rb ratios of fluids according to the contrasting fractionation behavior of Rb and Cs relative to K. Consequently, these ratios will also vary in fluids released by dehydration of phengitic micas. Although phengite is stable to pressures of 10 GPa, corresponding to depths of about 300 km (Schmidt, 1996; Domanik and Holloway, 1996), a K-rich fluid is continuously released during the subducting process due to the reaction phengite = K-rich omphacite + enstatite + coesite + K-rich fluid (Schmidt, 1996). Within an open system, each portion of produced fluid is immediately transported into the overlying mantle wedge. In other words, the fluid is distilled from the slab and LIL elements will be fractionated due to their different partitioning behavior between remaining phengite and fluid.

Assuming perfect Rayleigh fractionation, the element ratios R (= Rb/K, Cs/K, Cs/Rb) of phengite and the coexisting fluid vary as a function of the fraction of remaining phengite (F) depending on K_D and the alkali element ratio R^0 of phengite at the beginning of the reaction. Matsubaya and Matsuo (1982) derived equation 3 for Raleigh distillation for abundance ratios

$$\left(\frac{R_{phe}}{R_{phe}^0}\right)\left(\frac{1+R_{phe}}{1+R_{phe}^0}\right)^{(1/K_D - 1)} = F^{(1/K_D - 1)}. \quad (3)$$

This equation may be simplified to

$$R_{phe} = \frac{1}{K_D} R_{phe}^0 \cdot F^{(1/K_D - 1)}, \quad (4)$$

because for R values close to 0, the second term on the left side of equation 3 is ~1. Phengites formed in subduction zones at high pressures generally have low Rb/K, Cs/K, and Cs/Rb ratios, <0.1 (Bebout et al., 1999). The resulting variations of R values for fluids

$$R_{fluid} = \frac{1}{K_D} \cdot R_{phe}, \quad (5)$$

and of the coexisiting phengites, based on the model of perfect Rayleigh fractionation and with our derived K_D values, are shown in Figure 4A. Any

deviation from ideal Rayleigh fractionation (batch equilibrium) would result in lowering the fractionation of alkalies. In our model, the Cs/K and Cs/Rb ratios continuously decrease and the Rb/K ratios increase for decreasing fractions F of phengite. The same variations of the alkali ratios are observed within island arcs as a function of the depth to the Benioff zone (Fig. 4B). Thus, variable alkali ratios in IAB at different distances from the trench corresponding to different depths to the Benioff zone may be due to a continuous decomposition of phengite within the slab during an ongoing subduction.

It is generally accepted that fluids derived from the subducting slab influence the trace element patterns of IAB. Despite the fact that slab-derived fluids may interact with peridotitic mantle during their transport through the wedge (e.g., Stolper and Newman, 1994), fluids must retain a major portion of their initial element signature. There is also strong evidence that sediments with high phengite abundances play an important role for the trace element budget of subduction-related fluids (e.g., Bailey, 1996; Plank and Langmuir, 1998; Bebout et al., 1999). Alkali ratios of IAB systematically vary with increasing depth to the Benioff zone (Fig. 4B). This zone, underlying the volcanic front, corresponds to pressures of 4–10 GPa and temperatures of 600–800 °C (depending on the thermal characteristics of the subduction zone), under which dehydration processes, including decomposition of phengitic mica, occur (Schmidt, 1996). The calculated variations of Rb/K, Cs/K, and Cs/Rb ratios (Fig. 4A), based on our experimental results, and assuming perfect Rayleigh fractionation during a continuous decomposition of phengite, agree very well with the observations in IAB (Fig. 4B). We therefore argue that cross-arc variations of alkali ratios in IAB are strongly controlled by the ongoing dehydration of phengitic mica during subduction until phengite is completely used up. We also propose that fluids released from the slab pass through the mantle wedge relatively unaltered with respect to their alkali content. However, extensive mantle metasomatism beneath island arcs (e.g., Gill, 1981; Stopler and Newman, 1994) might lead to the formation of further alkali-bearing minerals, such as micas and amphiboles. Precipitation of these minerals might drastically alter the alkali budget within the mantle wedge. As determined by Melzer et al. (1998) and Melzer and Wunder (1999), phlogopite and richterite have contrasting exchange coefficients of K_D^{Rb-K} (phlogopite-fluid) = 2.5 and of K_D^{Rb-K} (richterite-fluid) = 0.5 at 2.0 GPa and 800 °C, respectively. Thus, the Rb/K ratio of the migrating fluid remains only unchanged, if both minerals (phlogopite and richterite) are absent or coexist.

TABLE 2. EXCHANGE COEFFICIENTS K_D
AND DISTRIBUTION COEFFICIENTS D
FOR PHENGITE - FLUID

Temperature [° C]	600	700
Pressure [GPa]	2	4
$K_D^{phe-fluid}$(Rb-K)	1.62 ± 0.10	1.84 ± 0.15
$K_D^{phe-fluid}$(Cs-K)	0.22 ± 0.06	0.37 ± 0.10
$K_D^{phe-fluid}$(Cs-Rb)	0.14 ± 0.05	0.20 ± 0.07
$D^{phe-fluid}$(Rb)	3.88 ± 0.04	4.41 ± 0.10
$D^{phe-fluid}$(Cs)	0.5 ± 0.2	0.9 ± 0.2

Figure 4. A: Calculated variations of Rb/K, Cs/K, and Cs/Rb ratios as function of fraction of remaining phengite assuming continuous dehydration reaction together with perfect Rayleigh fractionation and using K_D values derived for 4 GPa and 700 °C (see Table 2). B: For comparison, correlations of Rb/K, Cs/K, and Cs/Rb ratios with depth to Benioff zone as observed in island-arc magmas are shown (data from Whitford, 1975; Bailey et al., 1989; Woodhead and Johnson, 1993; Ryan et al., 1995).
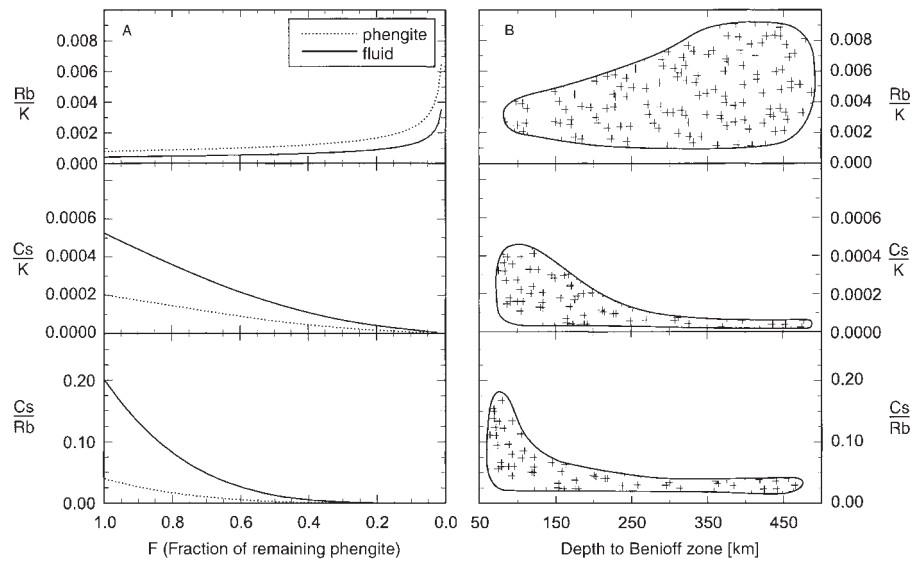
Keppler (1996) determined that the partitioning coefficients for Rb and K between silicic melt and an aqueous chloridic fluid are nearly equal. This indicates that fluids will have an almost similar alkali element signature as a coexisting melt in the source region of IAB. Therefore, based on our model, the varying alkali element compositions in arc basalts may be explained by one step, i.e., the ongoing decomposition of phengite and the simultaneous fluid-phengite alkali fractionation during the subduction process. In contrast, Ayers (1998) suggested a four-step model, the reliability of which depends on several somewhat arbitrary chosen parameters, including the fraction of free fluid in the slab and the melt fraction in the source region of IAB. A further disadvantage of Ayer's model is that his calculated trace element budget of fluid released from the slab is based on partition coefficients between fluid and model eclogite. However, this model assemblage of minerals lacks H_2O-bearing minerals, which may act as a source for free fluid within the slab.

CONCLUSIONS

The trends of alkali ratios in lavas erupted at convergent plate margins are due to compositional variations in fluids released from the subducting slab. Compositions of these hydrous fluids reflect their sedimentary origin and will modify the alkali element budget of melts in the source region of IAB. The results of our study indicate that the fluid produced by the breakdown of phengite within a subducting slab may pass through the mantle wedge into the subduction-related magma, without any large changes in its alkali ratios. However, any formation of LIL-containing hydrous phases such as phlogopite or richterite within the mantle wedge during the descent of the fluid would drastically alter the alkali content of the fluid due to their different K_D values (Melzer et al., 1998; Melzer and Wunder, 1999) compared to those of the system phengite-fluid.

REFERENCES CITED

Ayers, J., 1998, Trace element modeling of aqueous fluid–peridotite interaction in the mantle wedge of subduction zones: Contributions to Mineralogy and Petrology, v. 132, p. 390–404.

Bailey, J.C., 1996, Role of subducted sediments in the genesis of Kurile-Kamchatka island arc basalts: Sr isotopic and element evidence: Geochemical Journal, v. 30, p. 289–321.

Bailey, J.C., Frolova, T.I., and Burikova, I.A., 1989, Mineralogy, geochemistry, and petrogenesis of Kurile-island arc basalts: Contributions to Mineralogy and Petrology, v. 102, p. 265–280.

Bebout, G.E., Ryan, J.G., Leeman, W.P., and Bebout, A.E., 1999, Fractionation of trace elements by subduction-zone metamorphism—Effect for convergent-margin thermal evolution: Earth and Planetary Science Letters, v. 171, p. 63–81.

Brenan, J.M., Shaw, H.F., Ryerson, F.J., and Phinney, D.L., 1995, Mineral-aqueous partitioning of trace elements at 900°C and 2.0 GPa: Constraints on the trace element chemistry of mantle and deep crustal fluids: Geochimica et Cosmochimica Acta, v. 59, p. 3331–3350.

Domanik, K.J., and Holloway, J.R., 1996, The stability and composition of phengitic muscovite and associated phases from 5.5 to 11 GPa: Implications for deeply subducted sediments: Geochimica et Cosmochimica Acta, v. 60, p. 4133–4150.

Gill, J., 1981, Orogenic andesites and plate tectonics: Berlin, Springer-Verlag, 390 p.

Hutchison, C.S., 1976, Indonesian active volcanic arc: K, Sr, and Rb variation with depth to the Benioff zone: Geology, v. 4, p. 407–408.

Keppler, H., 1996, Constraints from partitioning experiments on the composition of subduction-zone fluids: Nature, v. 380, p. 237–240.

Matsubaya, O., and Matsua, S., 1982, Limitation to the application of Rayleigh distillation: Geochemical Journal, v. 16, p. 149–156.

Melzer, S., and Wunder, B., 1999, Experimentally determined K-Rb-Cs exchange coefficients between micas, amphiboles and aqueous chloride solutions between 0.2 and 4 GPa: Eos (Transactions, American Geophysical Union), v. 80, p. 361.

Melzer, S., Gottschalk, M., and Heinrich, W., 1998, Experimentally determined partitioning of Rb between richterites and aqueous chloride solutions: Contributions to Mineralogy and Petrology, v. 133, p. 315–328.

Plank, T., and Langmuir, C.H., 1998, The chemical composition of subducting sediment and its consequences for the crust and mantle: Chemical Geology, v. 145, p. 325–394.

Ryan, J.G., Morris, J., Tera, F., Leeman, W.P., and Tsvetkov, A., 1995, Cross-arc geochemical variations in the Kurile arc as a function of slab depth: Science, v. 270, p. 625–627.

Schmidt, M.W., 1996, Experimental constraints on recycling of potassium from subducted oceanic crust: Science, v. 272, p. 1927–1930.

Stalder, R., Foley, S.F., Brey, G.P., and Horn, I., 1998, Mineral-aqueous fluid partitioning of trace elements at 900–1200 °C and 3.0–5.7 GPa: New experimental data for garnet, clinopyroxene, and rutile, and implications for mantle metasomatism: Geochimica et Cosmochimica Acta, v. 62, p. 1781–1801.

Stolper, E., and Newman, S., 1994, The role of water in the petrogenesis of Mariana trough magmas: Earth and Planetary Science Letters, v. 121, p. 293–325.

Tatsumi, Y., 1986, Formation of the volcanic front in subduction zones: Geophysical Research Letters, v. 13, p. 717–720.

Whitford, D.J., 1975, Strontium isotopic studies of the volcanic rocks of the Sunda arc, Indonesia, and their petrogenetic implications: Geochimica et Cosmochimica Acta, v. 39, p. 1287–1302.

Woodhead, J.D., and Johnson, R.W., 1993, Isotopic and trace-element profiles across the New Britain island-arc, Papua New Guinea: Contributions to Mineralogy and Petrology, v. 115, p. 479–491.

Wunder, B., Andrut, M., and Wirth, R., 1999, High-pressure synthesis and properties of OH-rich topaz: European Journal of Mineralogy, v. 11, p. 803–813.

Zimmermann, R., Gottschalk, M., Heinrich, W., and Franz, G., 1997, Experimental Na-K distribution between amphiboles and aqueous chloride solutions, and a mixing model along the richterite–K-richterite join: Contributions to Mineralogy and Petrology, v. 126, p. 252–264.